Available online at www.sciencedirect.com
SCIENCE DIRECT
Polymer 46 (2005) 1949–1955
polymer
www.elsevier.com/locate/polymer

# Non-isothermal crystallisation kinetics of self-assembled polyvinylalcohol/silica nano-composite

Zheng Peng[a], L.X. Kong[a,*], Si-Dong Li[b]

[a]*Centre for Advanced Manufacturing Research, University of South Australia, Mawson Lakes, SA 5095, Australia*
[b]*College of Science, Zhanjiang Ocean University, Zhanjiang 524088, People's Republic of China*

Received 7 October 2004; received in revised form 6 December 2004; accepted 9 December 2004
Available online 19 January 2005

**Abstract**: A novel polyvinylalcohol/silica (PVA/$SiO_2$) nano-composite is prepared with the self-assembly monolayer (SAM) technique. The $SiO_2$ nano-particles are homogenously distributed throughout the PVA matrixes as nano-clusters with an average diameter ranged from 15 to 240 nm depending on the $SiO_2$ contents. Using differential scanning calorimetry (DSC), the non-isothermal crystallisation behaviour and kinetics of the PVA/$SiO_2$ nano-composites are investigated and compared to those of the pure PVA. There are strong dependences of the degree of crystallinity ($X_c$), peak crystallisation temperature ($T_p$), half time of crystallisation ($t_{1/2}$), and Ozawa exponent ($m$) on the $SiO_2$ content and cooling rate. The crystallisation activation energy ($E$) calculated with the Kissinger model is markedly lower when a small amount of $SiO_2$ is added, then gradually increases and finally becomes higher than that of the pure PVA when there is more than 10% $SiO_2$ in the composite.
© 2004 Elsevier Ltd. All rights reserved.

*Keywords:* Polyvinylalcohol; Nano-composite; Nonisothermal crystallisation

## 1. Introduction

Since polyvinylalcohol (PVA) was invented by Herrmann in 1924, its application has mainly been focused on fibre industry. Recently, it has received much attention in non-fibre applications specifically in pharmaceutical, biomedical and biochemical applications, due to its many desirable characteristics, such as biocompatibility, biodegradability, and water-solubility. PVA has been used for membranes [1,2], drug delivery system [3,4], and artificial biomedical devices [5,6].

However, the miserable solvent resistance, poor anti-ageing property, and insufficient mechanical properties of the PVA have restricted its further applications. To improve PVA's properties, the conventional method is to blend PVA with other materials [7–9]. Development of PVA-based nano-composites has been an emerging method to improve PVA's properties and many PVA-based nano-composites have recently been developed for different applications. For instance, Li et al. [10] prepared an intercalated nano-composite with improved thermal properties using magnesium, aluminium layered double hydroxide and PVA through exfoliation-adsorption technique. Xu et al. [11] developed a low-cost PVA/vermiculite (VMT) nano-composite to reinforce PVA. Lopez et al. [12] synthesised a new magnetically-soft and free-rotor PVA-based nano-composite with optimal thermal and mechanical properties for sensor and transformer applications. Peng et al. [13,14] recently synthesised a novel PVA/silica nano-composite by employing electrostatic attractive and hydrogen bonding interactions as the driving forces, which has improved thermal, mechanical, and solvent resistant properties and has great potential for biomedical and biochemical applications.

The crystallisation behaviour of polymer materials is crucial, because it ultimately governs its thermal properties, impact resistance and stress–strain property. Understanding the crystallisation property is significant to tailor the properties of final PVA products. The crystallisation of PVA is drastically affected by the tacticity of main chain [15], molecular weight [16] and plasticizer amount [17]. As

* Corresponding author. Tel.: +61 8 8302 5117; fax: +61 8 8302 5292.
*E-mail address:* lingxue.kong@unisa.edu.au (L.X. Kong).

0032-3861/$ - see front matter © 2004 Elsevier Ltd. All rights reserved.
doi:10.1016/j.polymer.2004.12.026

actual processing of polymer more likely involves a rate dependent crystallisation [18], the non-isothermal crystallisation behaviour and kinetics of PVA/silica composite will be studied in this work.

## 2. Experimental

### 2.1. Materials

Polyvinylalcohol (PVA) (average molecular weight: 67,000; polymerisation degree: 1400; hydrolysis rate: 86.7–88.7 mol%), silica nano-particles (average diameter: 14 nm; surface area: $200 \pm 25$ $m^2/g$) and polyallylamine hydrochloride (PAH) (average molecular weight: 70,000) were purchased from Sigma-Aldrich. All experimental materials were used as received.

### 2.2. Preparation of PVA/$SiO_2$ nano-composites [13]

The scheme of self-assembly monolayer nano-composite process (SAMN) developed is shown in Fig. 1 [13]. Firstly, the $SiO_2$ nano-particle aqueous dispersion is treated with an ultrasonic vibrator and its pH value is adjusted to 10 so as to negatively charge the $SiO_2$ nano-particles, which act as templates to adsorb positively charged polyallylamine hydrochloride (PAH) molecular chains through electrostatic adsorptive interaction. PVA molecular chains are then assembled on the surface of $SiO_2$ nano-particles through hydrogen bonding between hydroxy groups of the PVA and amino groups of the PAH. Finally, the treated $SiO_2$ nano-particles are uniformly dispersed in bulk PVA matrix, which is casted in a polytetrafluorethylene Petri dish, and dried in a vacuum oven to obtain PVA/$SiO_2$ nano-composite film.

### 2.3. SEM and TEM measurements

The scanning electron micrographs (SEM) of the composite were taken with a Philips XL30-EDAX instrument (USA). The fracture surface was obtained by splitting bulk samples quenched in liquid nitrogen. A sputter coater was used to pre-coat conductive gold onto the fracture surface before the observation. Thin film for transmission electron microscopy (TEM) was prepared by dropping the aqueous dispersion of nano-composite onto a copper grid coated with a carbon film. TEM measurement was done on a JEM-100CXII instrument (JEOL Ltd Japan) at an accelerating voltage of 100 kV.

### 2.4. Non-isothermal DSC analysis

Differential scanning calorimetry (DSC) analysis was performed on a Perkin–Elmer Pyris-1 system (USA) under nitrogen flow. The samples weighing between 10 and 12 mg were packed in the aluminium DSC pans and placed in the DSC cell. The samples were heated from 50 to 200 °C at a heating rate of 20 °C/min and kept at 200 °C for 10 min in order to destroy any nuclei that might act as seed crystals. Then, the samples were cooled down to 100 °C at a constant rate of 2.5, 5, 10, 20 and 30 °C/min, respectively.

## 3. Results and discussion

### 3.1. Distribution of $SiO_2$ nano-particles in PVA matrixes

The $SiO_2$ nano particles are not assembled in the composite as individual particles but as clusters of particles (Fig. 2). The number of nano particles in a cluster depends on the content of $SiO_2$ added. As the average diameter of the

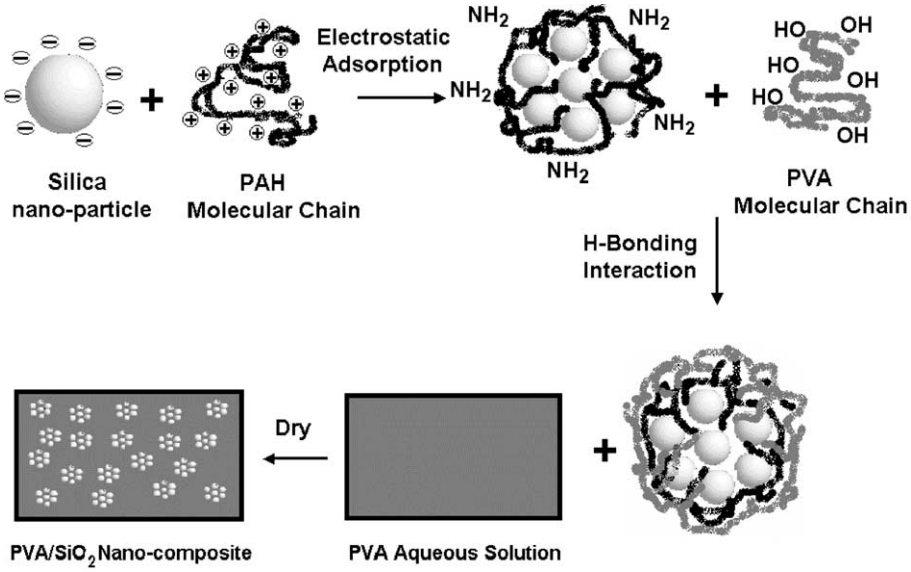


Fig. 1. The schematic of PVA/$SiO_2$ nano-composite process [13].

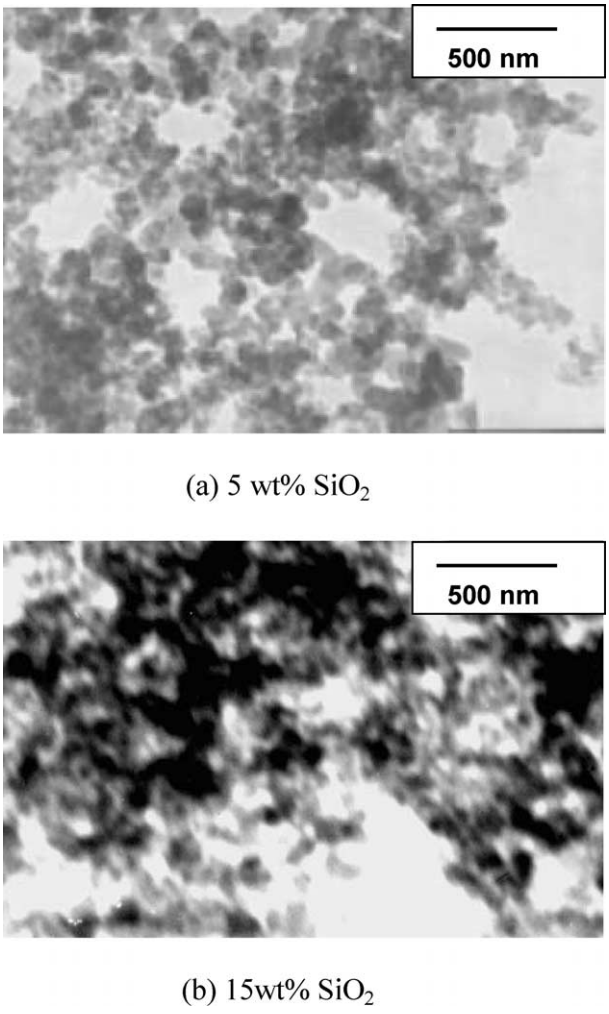


Fig. 2. Micrographs of the PVA/$SiO_2$ nano-composites (TEM).

$SiO_2$ nano-particles employed is just 14 nm, a complete PAH or PVA molecular chain is longer than the circumference of a single particle and is able to assemble more than one $SiO_2$ nano particle.

The average size of the $SiO_2$ clusters in nano composites with particle content of 0.5 to 15 wt% is shown in Fig. 3 after measuring more than 300 particles in three different TEM micrographs for every nano-composite. The average size is less than 30 nm when $SiO_2$ content is below 5 wt%, indicating a $SiO_2$ cluster has only quite a few primary nano-particles. However, at $SiO_2$ contents of 10 and 15 wt%, the size of the $SiO_2$ clusters is 100 and 240 nm, respectively, which suggests that when the $SiO_2$ content is higher than a certain level, nano particles will aggregate.

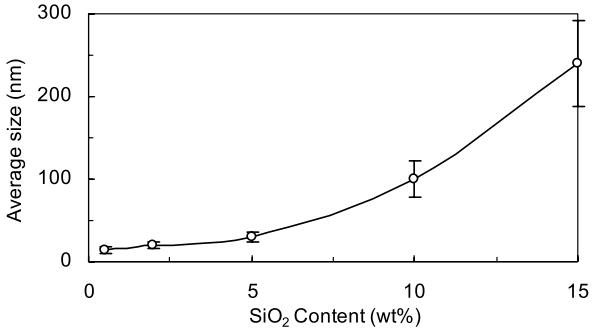


Fig. 3. Average size of $SiO_2$ clusters in PVA/$SiO_2$ nano-composites.

### 3.2. Non-isothermal crystallisation behaviour of PVA/$SiO_2$ nano-composites

Fig. 4 shows the DSC curves of pure PVA and PVA/$SiO_2$ nano-composite with a $SiO_2$ content of 5 wt% in nitrogen atmosphere for five different cooling rates, respectively. The DSC curves of the pure PVA and prepared nano-composites are similar, and there is only one obvious crystallisation enthalpy peak between 130 and 170 °C, showing the crystallisation behaviour of the pure PVA and prepared nano-composites are analogous. In both cases, the crystallisation enthalpy peak shifts to a lower temperature with an increasing cooling rate. Therefore, the lower the cooling rate, the easier the crystallisation.

However, the peak crystallisation temperature ($T_p$) corresponding to the crystallisation enthalpy peak (Fig. 4) is lower at a higher $SiO_2$ content and a higher cooling rate (Fig. 5), even though the effect at $SiO_2$ contents less than 2 wt% is not significant. When specimens are cooled down at a high cooling rate, the motion of PVA molecular chains cannot follow the cooling temperature in time due to the influence of heat hysteresis, which leads to a lower peak crystallisation temperature. When $SiO_2$ particles are added into the PVA matrices, the particle clusters act as a heat

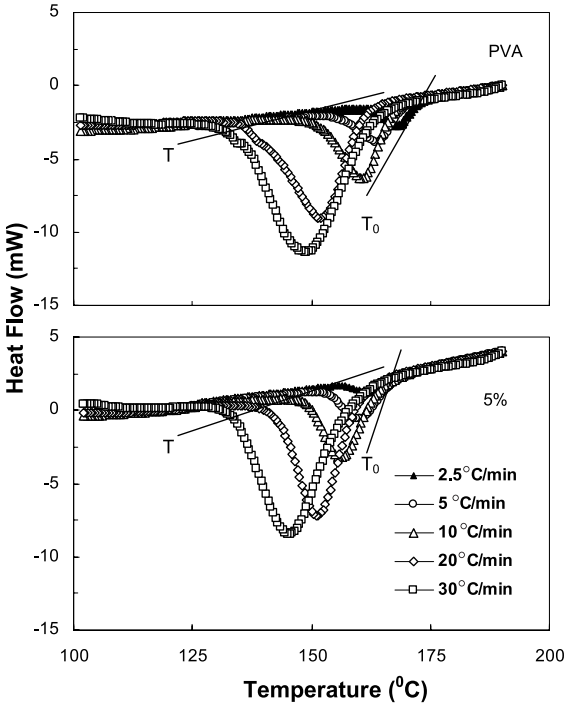


Fig. 4. DSC thermograms of the pure PVA and nano-composite (5 wt%) at various cooling rates.

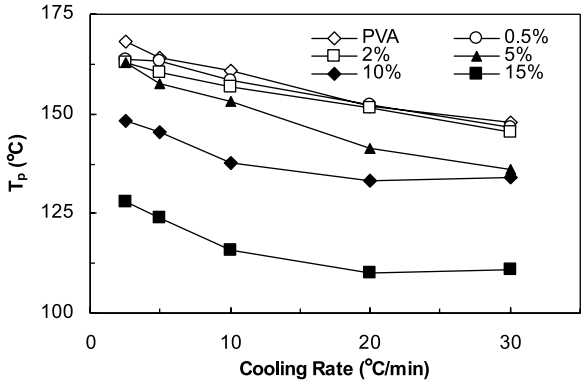


Fig. 5. Relation between $T_p$ and cooling rate.

barrier preventing the heat transfer among the PVA molecular chains and consequently, the crystallisation occurs at a lower temperature when the $SiO_2$ content is high.

The degree of crystallinity ($X_c$) can be obtained from the enthalpy evolved during crystallisation using the following equation [19]:

$$X_c(\%) = \frac{\Delta H_c}{(1-\varphi)\Delta H_m} 100 \quad (1)$$

where $\Delta H_c$ is the apparent enthalpy of crystallisation, $\Delta H_m$ is the extrapolated enthalpy corresponding to the melting of a 100% crystalline sample with an average value of 138.6 J/g [20], and $\varphi$ is the weight fraction of $SiO_2$ nano particles in the composites. The $X_c$ increases dramatically at a low cooling rate (2.5–10 °C/min), while it is relatively stable when the cooling rate is higher (20–30 °C/min) (Table 1). Therefore, the cooling rate is a major factor to affect the $X_c$ at low cooling rates.

$SiO_2$ content is another major factor to affect the $X_c$. There is a maximum $X_c$ at the $SiO_2$ content of 0.5 wt% for all cooling rates. As the $SiO_2$ content increases, $X_c$ decreases significantly (Table 1). Therefore, the introduction of a small amount of $SiO_2$ (0.5 wt%) into PVA can accelerate the crystallisation while a large amount of $SiO_2$ will restrict the crystallisation.

### 3.3. Non-isothermal crystallisation kinetics of PVA/$SiO_2$ nano-composites

The relative degree of crystallinity, $X_T$, as a function of crystallisation temperature can be calculated using the following equation [21]:

$$X_T = \frac{\int_{T_0}^{T} \left(\frac{dH}{dt}\right) dt}{\int_{T_0}^{T_\infty} \left(\frac{dH}{dt}\right) dt} \quad (2)$$

where $T_0$ and $T_\infty$ are the starting and finishing crystallisation temperatures taken at the starting and finishing inflections of the crystallisaion peak (Fig. 4), respectively, $H$ is the enthalpy of the process. After substituting the areas of the DSC curves, Eq. 2 becomes

$$X_T = \frac{A_T}{A_\infty} \quad (3)$$

where $A_T$ is the area under the DSC curves from $T=T_0$ to $T=T$ and $A_\infty$ is the total area under the crystallisation curve. Based on this equation, $X_T$ at a specific temperature can be calculated (Fig. 6). During non-isothermal crystallisation, the crystallisation time has the relation with crystallisation temperature:

$$t = \frac{(T_0 - T)}{\beta} \quad (4)$$

where $T$ is the temperature at crystallisation time $t$, and $\beta$ is the cooling rate. Combining Eqs. (2) and (4), Fig. 6 can be changed into Fig. 7, where the relative degree of crystallinity, $X_t$, which is a function of the crystallisation time, is presented as a function of crystallisation time. It can be seen that at a higher cooling rate, it takes less time for crystallisation to complete. As the effect of retardation on crystallisation, all curves have approximately an S (or reversed S) shape. At the later stage, the curves tend to become flat due to the spherulite impingement [22].

From Fig. 7, the half time for completing crystallisation ($t_{1/2}$) can be estimated (Fig. 8). There is a minimum $t_{1/2}$ at $SiO_2$ content of 0.5 wt%. With an increasing $SiO_2$ content, $t_{1/2}$ increases gradually. At a relatively low $SiO_2$ content, the $SiO_2$ clusters cannot restrict the motion of the PVA molecular chains, but act as heterogeneous nucleating agent during non-isothermal crystallisation process, and, therefore, accelerate the crystallisation. While at a higher $SiO_2$ content, the $SiO_2$ clusters act as a barrier that restricts the thermal motion of PVA molecular chains, and, therefore, retard the formation of crystals. As a result, the

Table 1
$X_c$ at various cooling rates for PVA and nano-composites

| $\beta$(°C/min) | $X_c$ (%) | | | | | |
|---|---|---|---|---|---|---|
| | PVA | 0.5% | 2% | 5% | 10% | 15% |
| 2.5 | 18.8 | 19.1 | 16.1 | 14.2 | 12.2 | 9.1 |
| 5 | 21.0 | 21.4 | 19.7 | 16.7 | 15.1 | 12.3 |
| 10 | 22.6 | 22.4 | 20.8 | 16.8 | 18.2 | 12.6 |
| 20 | 23.5 | 24.9 | 20.6 | 20.8 | 19.1 | 12.2 |
| 30 | 24.9 | 25.8 | 21.2 | 20.8 | 19.3 | 13.4 |

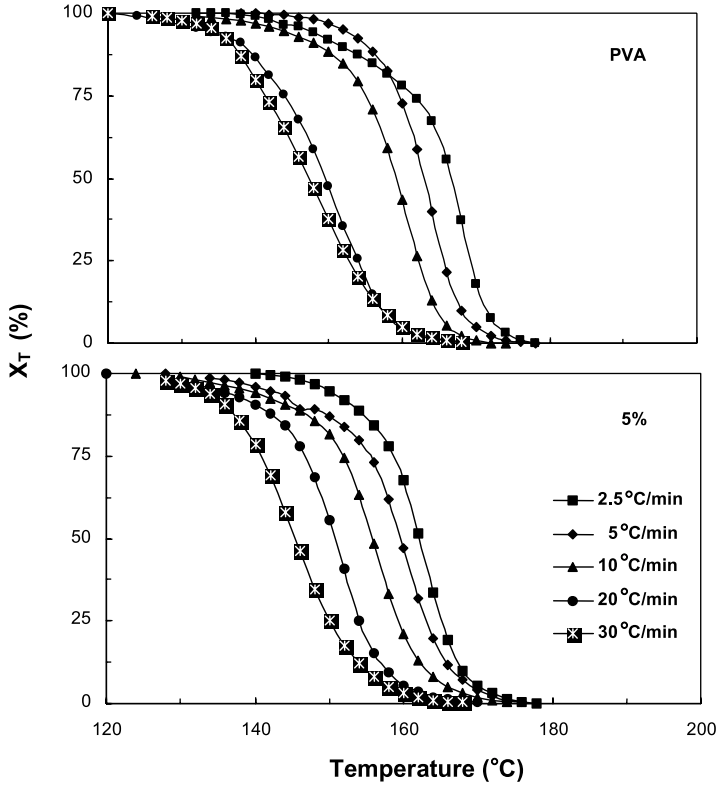


Fig. 6. Dependence of $X_T$ on crystallisation temperature and cooling rate for PVA and nano-composite (5 wt%).

addition of a large amount of $SiO_2$ nano-particles can delay the overall crystallisation process.

Although many models have been developed for isothermal crystallisation kinetics, only the models from Jeziorny [23], Ziabicki [17,24], and Ozawa [22] are suitable for non-isothermal kinetics. In the present study, the Ozawa equation

$$1 - X_T = \exp \frac{-k_T}{\beta^m} \tag{5}$$

is adopted to investigate the non-isothermal crystallisation of the pure PVA and PVA/$SiO_2$ nano-composites at various cooling rate and is extended from the Avrami equation which was originally for isothermal crystallisation,

$$1 - X_t = \exp(-kt^n) \tag{6}$$

to non-isothermal crystallisation by assuming that the sample is cooled at a constant cooling rate. Here $X_t$ and $X_T$ are relative degree of crystallinity as a function of

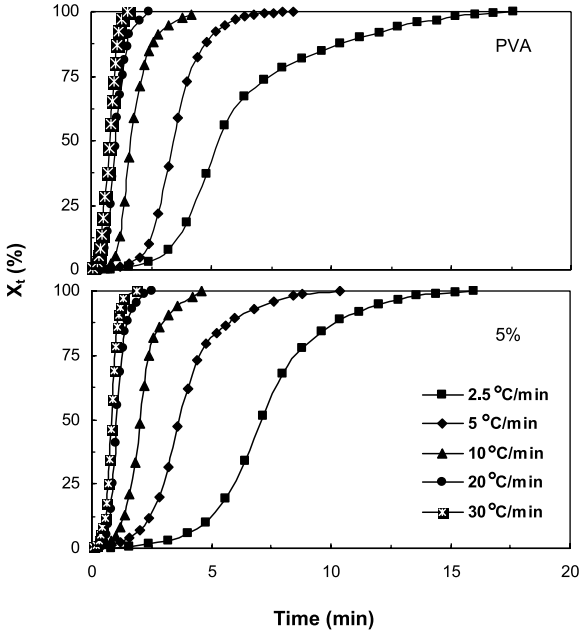


Fig. 7. Dependence of $X_t$ on crystallisation time and cooling rate for PVA and nanocompsote (5 wt%).

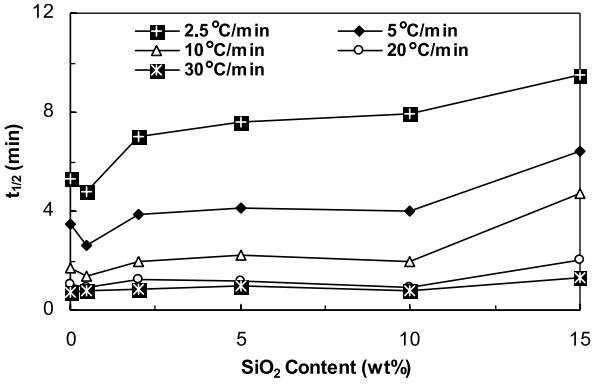


Fig. 8. Variation of $t_{1/2}$ with silica content at various cooling rates.

crystallisation time and temperature, respectively, $k$ is the crystallisation kinetics rate constant, $k_T$ is the cooling function of non-isothermal crystallisation at temperature $T$, $t$ is crystallisation time, $\beta$ is the cooling rate, $n$ is the isothermal Avrami exponent, and $m$ is the Ozawa exponent depending on the dimension of crystal growth. Eq. 5 can be linearised as follows:

$$\ln[-\ln(1-X_T)] = \ln k_T - m \ln \beta \quad (7)$$

The Ozawa equation can be used to analyze the non-isothermal crystallisation process, as the Ozawa equation possesses a good linearity (Fig. 9). The intercept and slope of $\ln[-\ln(1-X_T)]$ versus $\ln\beta$ yield $k_T$ and $m$, respectively (Table 2).

The $m$ for PVA varies between 0.52 and 0.98 for a temperature between 146–154 °C. For the nano-composite with $SiO_2$ content of 5 wt%, the $m$ is between 1.14 and 1.53 for the same temperature range of 154–164 °C. The $k_T$ for PVA is relatively stable, while it decreases significantly from 8.60 to 2.14 for nano-composite with 5 wt% $SiO_2$ when the crystallisation temperature increases from 154 to 164 °C. The fluctuation of $m$ and $k_T$ can be attributed to the complexity of dynamic crystallisation process as a function of crystallisation time and temperature. The $m$ and $k_T$ for nano-composite are obviously different from those of the pure PVA, suggesting that the presence of $SiO_2$ nano-particles greatly influence the growth of crystals.

The crystallisation activation energy ($E$) can be calculated by using Kissinger equation [25–27]:

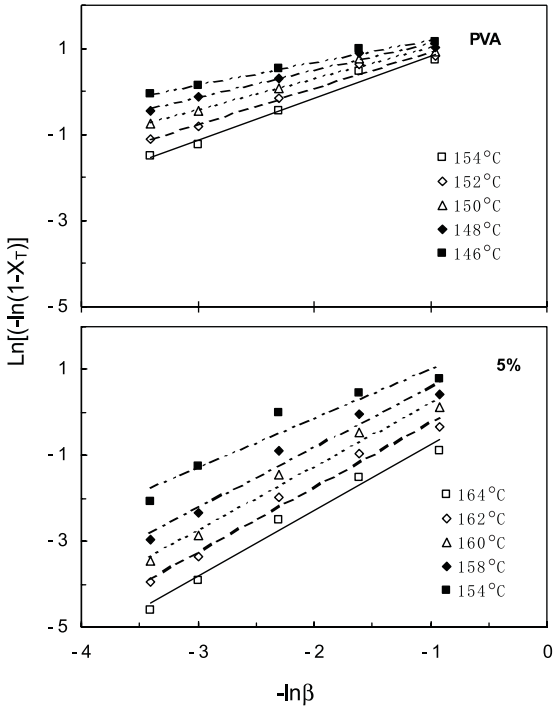


Fig. 9. Ozawa plots of $\ln[-\ln(1-X_T)]$ versus $-\ln\beta$ for PVA and nano-composite 5%.

Table 2
Ozawa parameter $m$ and cooling function $K_T$ for PVA and nano-composite (5 wt%)

| Sample | $T$ (°C) | $m$ | $K_T$ |
|---|---|---|---|
| PVA | 146 | 0.52 | 5.62 |
| | 148 | 0.63 | 5.74 |
| | 150 | 0.73 | 5.62 |
| | 152 | 0.85 | 5.95 |
| | 154 | 0.98 | 6.13 |
| Nano-composite 5% | 154 | 1.14 | 8.60 |
| | 158 | 1.41 | 7.41 |
| | 160 | 1.50 | 5.74 |
| | 162 | 1.52 | 3.63 |
| | 164 | 1.53 | 2.14 |

$$E = \frac{d[\ln(\beta/T_p^2)]}{d(1/T_p)}R \quad (8)$$

where $R$ is the universal gas constant, $\beta$ is the cooling rate, and $T_p$ is the peak crystallisation temperature. Having plotted $\ln(\beta/T_p^2)$ versus $1/T_p$, the crystallisation activation energy $E$ can be obtained (Fig. 10). The $E$ of the nano-composites decreases markedly when $SiO_2$ content increases from 0 to 0.5 wt%, then gradually increases when $SiO_2$ content increases further, and finally becomes higher than that of the pure PVA when $SiO_2$ content is higher than 10 wt%. This confirms that the $SiO_2$ nano-particles act as heterogeneous nuclei and accelerate the crystallisation process at a relatively low $SiO_2$ content. While at a higher $SiO_2$ content, the $SiO_2$ clusters act as a barrier to retard the crystallisation by depressing the crystal growth because of the interaction between $SiO_2$ clusters and PVA matrixes.

## 4. Conclusions

The self-assembly monolayer nano-composite process (SAMN) has successfully been used to prepare a poly-vinylalcohol/silica nano-composite, in which the $SiO_2$ nano-particles are uniformly distributed throughout PVA matrixes as nano clusters. At a low $SiO_2$ content, the

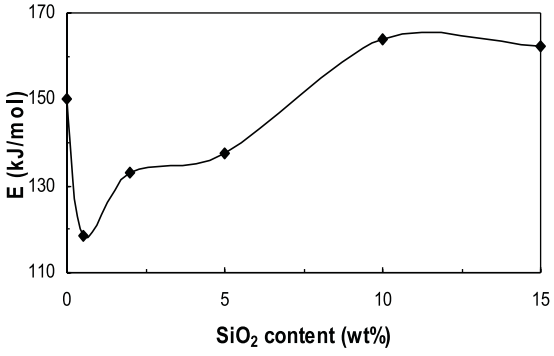


Fig. 10. Variation of crystallisation activation energy $E$ with $SiO_2$ content.

crystallisation of nano-composite is accelerated, while at a higher content, its crystallisation is retarded. The crystallinity degree of the nano-composites decreases with an increasing $SiO_2$ content, but increases with the cooling rate. The peak crystallisation temperature decreases with the cooling rate and $SiO_2$ content. The half time of crystallisation decreases with the cooling rate, but increases with the $SiO_2$ content. The Ozawa parameter $m$ and cooling function $k_T$ change with the crystallisation temperature and an addition of $SiO_2$ nano-particles. The crystallisation activation energy becomes markedly lower when a small amount of $SiO_2$ is added, then gradually increases and finally becomes higher than that of the pure PVA when more than 10 wt% of $SiO_2$ is added.

## Acknowledgements

The authors would like to acknowledge Dr P. Spiridonov at University of South Australia for his helpful comments. The project has been supported by UniSA Emerging Thematic Priority Fund and UniSA University President Scholarship.

## References

[1] Da Silva E, Lebrun L, Metayer M. Polymer 2002;43(19):5311.
[2] Chuang WY, Young TH, Chiu WY, Lin CY. Polymer 2000;41(15):5633.
[3] Brazel CS, Peppas NA. Polymer 1999;40(12):3383.
[4] Oh KS, Han SK, Choi YW, Lee JH, Lee JY, Yuk SH. Biomaterials 2004;25(12):2393.
[5] Young TH, Chuang WY, Hsieh MY, Chen LW, Hsu JP. Biomaterials 2002;23(16):3495.
[6] Kobayashi M, Toguchida J, Oka M. Biomaterials 2003;24(4):639.
[7] Jang JS, Lee DK. Polymer 2004;45(5):1599.
[8] Yi JZ, Goh SH. Polymer 2003;44(6):1973.
[9] Park JS, Park JW, Ruckenstein E. Polymer 2001;42(9):4271.
[10] Li BG, Hu Y, Zhang R, Chen ZY, Fan WC. Mater Res Bull 2003;38(11–12):1567.
[11] Xu J, Meng YZ, Li RKY, Xu Y, Rajulu AV. J Polym Sci, Polym Phys 2003;41(7):749.
[12] Lopez D, Cendoya I, Torres F, Tejada J, Mijangos C. J Appl Polym Sci 2001;82(13):3215.
[13] Peng Z, Kong LX, Li SD. J Appl Polym Sci 2004 in press.
[14] Kong LX, Peng Z. Key Eng Mat 2004 in press.
[15] Yoshitaka N, Nakano T, Okamoto Y, Gotoh Y, Nagura M. Polymer 2001;42(24):9679.
[16] Ikejima T, Yoshie N, Inoue Y. Polym Degrad Stab 1999;66(2):263.
[17] Jang J, Lee DK. Polymer 2003;44(26):8139.
[18] Weng W, Chen G, Wu D. Polymer 2003;44(26):8119.
[19] Liu XH, Wu QJ, Berglund LA, Qi ZN. Macromol Mater Eng 2002;287(8):515.
[20] Peppas NA, Merrill EW. J Polym Sci, Pol Chem 1976;14(2):441.
[21] Hammami A, Spruiell JE, Mehrotra AK. Polym Eng Sci 1995;35(10):797.
[22] Ozawa T. Polymer 1971;12(3):150.
[23] Jeziorny A. Polymer 1978;19(10):1142.
[24] Liu MY, Zhao QX, Wang Y, Zhang CG, Mo ZS, Cao SK. Polymer 2003;44(8):2537.
[25] Kim SH, Ahn SH, Hirai T. Polymer 2003;44(19):5625.
[26] Papageorgiou GZ, Karayannidis GP. Polymer 2001;42(6):2637.
[27] Yan HQ, Chen S, Qi GR. Polymer 2003;44(26):7861.